

3D cloud products for weather prediction and climate modelling

Autor(en): **Seiz, Gabriela / Baltsavias, Emmanuel P. / Gruen, Armin**

Objektyp: **Article**

Zeitschrift: **Geographica Helvetica : schweizerische Zeitschrift für Geographie = Swiss journal of geography = revue suisse de géographie = rivista svizzera di geografia**

Band (Jahr): **58 (2003)**

Heft 2: **Beiträge zur Forschung in der Schweizerischen Fernerkundung = Contributions to Swiss remote sensing research = Contributions à la recherche de télédétection suisse**

PDF erstellt am: **22.07.2024**

Persistenter Link: <https://doi.org/10.5169/seals-872890>

Nutzungsbedingungen

Die ETH-Bibliothek ist Anbieterin der digitalisierten Zeitschriften. Sie besitzt keine Urheberrechte an den Inhalten der Zeitschriften. Die Rechte liegen in der Regel bei den Herausgebern.

Die auf der Plattform e-periodica veröffentlichten Dokumente stehen für nicht-kommerzielle Zwecke in Lehre und Forschung sowie für die private Nutzung frei zur Verfügung. Einzelne Dateien oder Ausdrucke aus diesem Angebot können zusammen mit diesen Nutzungsbedingungen und den korrekten Herkunftsbezeichnungen weitergegeben werden.

Das Veröffentlichen von Bildern in Print- und Online-Publikationen ist nur mit vorheriger Genehmigung der Rechteinhaber erlaubt. Die systematische Speicherung von Teilen des elektronischen Angebots auf anderen Servern bedarf ebenfalls des schriftlichen Einverständnisses der Rechteinhaber.

Haftungsausschluss

Alle Angaben erfolgen ohne Gewähr für Vollständigkeit oder Richtigkeit. Es wird keine Haftung übernommen für Schäden durch die Verwendung von Informationen aus diesem Online-Angebot oder durch das Fehlen von Informationen. Dies gilt auch für Inhalte Dritter, die über dieses Angebot zugänglich sind.

3D Cloud Products for Weather Prediction and Climate Modelling

Gabriela Seiz, Emmanuel P. Baltasvias, Armin Gruen, Zurich

1 Introduction

The EU-FP4 project Cloudmap aimed to estimate new cloud-top products (heights, type, optical thickness, effective droplet size), especially for cirrus and contrail clouds from existing and new sensors, using three different techniques (brightness temperature with CO₂ slicing method, stereo-scopic and Oxygen A-band). These cloud-top products were validated using airborne sensor underflights, multi-resolution contemporaneous observations from space sensors and ground-based remote sensing instruments. Cloudmap ended in January 2001 and is now continued by the EU-FP5 project Cloudmap2.

Cloudmap2 aims to produce and exploit value-added remote sensing data products on macroscopic (e.g. cloud-top height) and microscopic (e.g. cloud droplet radius) properties and water vapour distributions in order to characterize sub-grid scale processes within Numerical Weather Prediction Models (NWP) through validation and data assimilation. Earth Observation (EO) data, provided by the European Space Agency (ESA), the European Organisation for the Exploitation of Meteorological Satellites (EUMETSAT) and the National Aeronautics and Space Administration (NASA) are used to derive geophysical value-added data products over Europe and the North Atlantic region, whenever possible in near real-time. Ground-based active (cloud radar, ceilometer) and passive (stereo imager system, IR camera) remote-sensing instruments are used to validate the EO-derived data to be merged with the satellite-based results for 3D representations of the clouds. Numerical simulation experiments based on state-of-the-art radiative transfer methods are used to quantify the effect of broken clouds on the Earth's radiation budget and lead to a better representation of clouds within NWP models.

The role of the ETH in Cloudmap and Cloudmap2 is to estimate cloud top height (CTH) and cloud top wind (CTW) from stereo images from satellites and cloud base height (CBH) and cloud base wind (CBW) from stereo images acquired by their own ground-based stereo imager system, with stereo-photogrammetric techniques. As a next step, the cloud top and cloud base results are combined and visualized in 3D.

This paper describes the CTH and CTW results with regard to the use of different stereo image resolutions (ATSR2, MISR, Meteosat-6/-7) and spectral wavelengths (ATSR2). Further, the CBH and CBW results from the new ground-based stereo imager system are presented, and the ground and satellite-based results are compared.

2 Satellite-based stereo analysis

Stereoscopy of clouds has a long tradition in satellite meteorology (HASLER 1981). Stereo measurements have the advantage that they depend only on basic geometric relationships of observations of cloud features from at least two different viewing angles, while other cloud top height estimation methods are dependent on the knowledge of additional cloud/atmosphere parameters like cloud emissivity, ambient temperature or lapse rate. From satellites, both geostationary and polar-orbiting sensors can be used in a number of configurations, as described in e.g. FUJITA (1982), CAMPBELL & HOLMLUND (2000), Yi et al. (2001). Over Europe, the following satellite configurations can be used for cloud stereoscopy:

- Single polar-orbiter with two views: ERS2-ATSR2, ENVISAT-AATSR, EOS Terra-ASTER
- Single polar-orbiter with more than two views: EOS Terra-MISR
- Two geostationary Meteosat satellites: Meteosat-6 and Meteosat-7

Further combinations, like a Meteosat satellite with another geostationary satellite (e.g. GOES-E), are not recommended due to the S-N scanning direction of the Meteosat satellites (while all other geostationary satellites are N-S scanning). The different scan directions additionally increase the difficulty for the matching of images and the motion error correction.

2.1 ATSR2

The ATSR2 instrument is part of the ERS-2 satellite system which was launched in April 1995. The successor sensor, AATSR, is part of the Envisat payload which was launched in spring 2002. ERS-2 is in a near-polar, sun-synchronous orbit at a mean height of 780 km, an inclination of 98.5° and has a sub-satellite velocity of 6.7 km/s. The spacecraft is positioned to operate with a descending equator crossing of around 10:30 local solar time. The repeat cycle is about 3 days. First, the ATSR2 views the surface along the direction of the orbit track at an incidence angle of 55° as it flies toward the scene. Then, some 120s later,

ATSR2 records a second observation of the scene at an angle close to the nadir (Fig. 1) (MUTLOW 1999). ATSR2's field of view comprises two 500 km-wide curved swaths, with 555 pixels across the nadir swath and 371 pixels across the forward swath. The pixel size is 1x1 km at the centre of the nadir scan and 1.5 x 2 km at the centre of the forward scan. The sensor records in 7 spectral channels: 0.55 μm , 0.67 μm , 0.87 μm , 1.6 μm , 3.7 μm , 10.8 μm and 12.0 μm , which is comparable to the channels of the new SEVIRI instrument on MSG. The geolocation for the rectified (GBT) products maps the acquired pixels onto a 512 x 512 grid with 1km pixel sizes. The axes of the grid are the ERS-2 satellite ground-track and great circles orthogonal to the ground-track.

2.1.1 Cloud top height retrieval

Our cloud top height retrieval from ATSR2 is based on the GBT data product. The 10-bit GBT data were first reduced to 8-bit and linearly stretched between the minimum and maximum value, cutting 0.5% on both sides of the histogram (excluding the pixels assigned with an error code). As no a priori values of the cloud heights are given to the matching algorithm, a hierarchical matching procedure with 3 pyramid levels is applied so that the maximum possible parallax at the highest level is only 1-2 pixels. Every pyramid level is enhanced and radiometrically equalized with a Wallis filter (WALLIS 1976). Points with good texture are selected with an interest operator (FÖRSTNER & GÜLCH 1987) in the first pyramid level because it is likely that the same points are well detectable also in the other levels. The matching was done with the Multi-Photo Geometrically Constrained Matching Software package developed at our institute (BALTSAVIAS 1991), which is based on Least-Squares-Matching (LSM) (GRÜN 1985). The matching solutions are quality-controlled with absolute and relative tests on the matching statistics. The resulting y-parallaxes are converted into cloud heights after PRATA & TURNER (1997), taking into consideration that the zenith angles have to be projected on the along-track plane.

The height values of the successfully matched points are finally interpolated to the 512x512 grid. Three cloud tests are applied on the ATSR2 data to separate cloud, land and mixed pixels: 1) 0.87 μm -11.0 μm -ratio test, 2) 11.0 μm -3.7 μm difference test and 3) 3.7 μm -12.0 μm difference test. If a pixel passed all three tests, it was classified as cloudy; if none of the tests were passed, the pixel was marked as land; all other pixels were classified as mixed. Only the cloudy pixels were then selected for further investigation. A quality control of the results of the mixed and land pixels showed that many blunders (i.e. wrongly matched points) could not be detected. This is caused by multiple solutions within the land surface at this

spatial resolution and by the problem that the matching result – especially at higher pyramid levels – is strongly affected by the near cloud borders.

2.1.2 Across-track wind retrieval and along-track wind error

The forward and nadir ATSR2 images are acquired with a mean time delay of 120 seconds so that significant cloud motion is observable between the two scans. Given no time delay, the following relationships are observed:

$$x_p = 0 \quad (2.1.)$$

$$y_p = f(\text{cloud top height, zenith angles})$$

with x_p : cross-track parallax, y_p : along-track parallax. Considering time delay and cloud motion, equation (2.1.) has to be modified as:

$$x_p = f(\text{cross-track wind}) = u'(t_{\text{nadir}} - t_{\text{forward}}) \quad (2.2.)$$

$$y_p = f(\text{cloud top height, zenith angles, along-track wind})$$

$$= H(\tan \theta_f - \tan \theta_n) + v'(t_{\text{nadir}} - t_{\text{forward}})$$

with u' : cross-track wind component (E-W), v' : along-track wind component (N-S)

For the cross-track wind retrieval and along-track wind correction, the exact time difference between the corresponding pixels in the forward and the nadir scan is calculated from the along-track distance on the ground and the satellite velocity according to LORENZ (1985). For the conical scanning of ATSR2, the time difference varies significantly across the scan. North winds lead to an underestimation of the heights so that the along-track wind component has to be added to the y-parallax while southerly winds result in cloud top heights that are too high.

As horizontal wind and cloud motion do not necessarily correspond, especially over mountainous terrain, it is not recommended to use wind data (e.g. from NWP model output) for the cloud motion error correction. A more reliable method is the use of cloud tracking information from geostationary satellites, as we showed in SEIZ & BALTSAVIAS (2000). For Switzerland, the following three possibilities are available:

- **Meteosat-6 5min Rapid Scans:** EUMETSAT supported the Mesoscale Alpine Programme (MAP) in autumn 1999 (Sep – Nov) by 5min rapid scans of the Alpine region (Fig. 1) with the in-orbit stand-by Meteosat-6 positioned at 9° W (EUMETSAT 2002). The limited scan starts at line 4218 (or line 2109 for IR/WV) of the operational Meteosat-7 scan which results in a time difference between the two scans of 1:05 minutes. The spatial resolution of the VIS channel is 2.5 x 2.5 km (5 x 5 km IR/WV) at the equator, with decreasing y-resolution towards the poles. Over Switzerland (47° N), the pixel size is approximately 2.5 x 4 km (or 5 x 8km for IR/WV).
- **Meteosat-6 10min Rapid Scans:** Following the

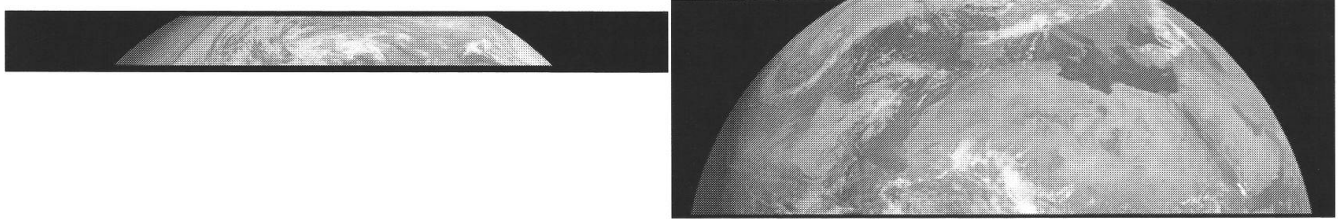


Figure 1: Scanning area of Meteosat-6 Rapid Scans; left: 5min Rapid Scans during MAP; right: 10min Rapid Scans

Meridionale Ausdehnung der Meteosat-6 Rapid Scans; links: 5min Rapid Scans während MAP; rechts: 10min Rapid Scans

Région des Meteosat-6 Rapid Scans; à gauche: 5min Rapid Scans pendant le programme MAP; à droite: 10min Rapid Scans

Photo: © EUMETSAT

success of the 5min Rapid Scanning support provided to the MAP experiment in 1999, new 10min Rapid Scans were started by EUMETSAT in August 2000. These trials normally lasted 48 to 72 hours a week. Since September 2001, an operational 10min Rapid Scanning Service (RSS) is maintained (EUMETSAT 2002). For the rapid scans, the in-orbit stand-by Meteosat-6 instrument, positioned at 9° W, is used. The limited scan consists of 5000 x 1666 pixels (or 2500 x 833 for IR/WV), starts at line 2947 (or line 1474 for IR/WV) of the operational Meteosat-7 scan and covers an area from approximately 10° to 70° N (Fig. 1). The time difference between Meteosat-6 and Meteosat-7 in this configuration is about 5 min.

- **Meteosat-7:** The operational European meteorological geostationary satellite, Meteosat-7, is located at 0°; the whole scan consists of 5000 x 5000 pixels (or 2500 x 2500 for IR/WV). The spatial resolution of the VIS channel is 2.5 x 2.5 km (5 x 5 km IR/WV) at the equator, with decreasing y-resolution towards the poles. Over Switzerland (47° N), the pixel size is approximately 2.5 x 4 km (or 5 x 8km for IR/WV).

For the tracking, the Meteosat images were preprocessed with a Wallis filter for contrast enhancement. The corresponding points in the image sequence were then determined with our LSM algorithm. For the 5min MAP Rapid Scans, only the original images were used in the matching, while for the 10 min Rapid Scans two pyramid levels (original + 1st pyramid level) and for the Meteosat-7 images four pyramid levels (original + 1st, 2nd and 3rd pyramid level) were taken. The disadvantage of the Meteosat-7 images against the 5min or 10min Meteosat-6 Rapid Scans is the increased difficulty to assign the Meteosat cloud motion to the corresponding cloud objects within the ATSR2 stereo pairs. Furthermore, the tracking is more difficult as the

shape of the clouds can change significantly within the 30min interval.

2.1.3 Wind correction for ATSR2 Stereo CTH

The Meteosat-6 and Meteosat-7 motion vectors were resampled to the 512 x 512 ATSR2 grid, and the cross-track and along-track components calculated. With the time difference between nadir and forward acquisition, the along-track components are converted into the CTH correction amounts. North winds lead to an underestimation of the heights so that the along-track wind component has to be added to the y-parallax while southerly winds result in cloud top heights that are too high. The cross-track component can be used as a comparison to the ATSR2 x-disparity field (scaled with height factor h); large discrepancies would indicate (matching/ tracking blunders excluded) geolocation errors of the ATSR2 images.

2.2 Multi-view polar-orbiting satellite: MISR

As an alternative to the logistically difficult problem of a tandem mission of two polar-orbiting satellites to get synchronous high-resolution stereo images, the use of at least three non-symmetric views from a single polar-orbiting satellite can solve the issue of cloud motion errors in satellite-based stereo CTH's, as it allows the simultaneous estimation of CTH and CTW. The only currently operational satellite to offer such multi-view stereo images is the Multi-angle Imaging Spectro Radiometer (MISR). MISR was launched aboard the EOS AM-1 Terra spacecraft in December 1999. The orbit is sun-synchronous at a mean height of 705km, with an inclination of 98.5° and an equatorial crossing time at about 10:30 a.m.. The repeat cycle is 16 days. The MISR instrument consists of nine pushbroom cameras at different viewing angles: -70.5° (named DA), -60.0° (CA), -45.6° (BA), -26.1° (AA), 0.0° (AN), 26.1° (AF), 45.6° (BF), 60.0° (CF) and 70.5° (DF). The

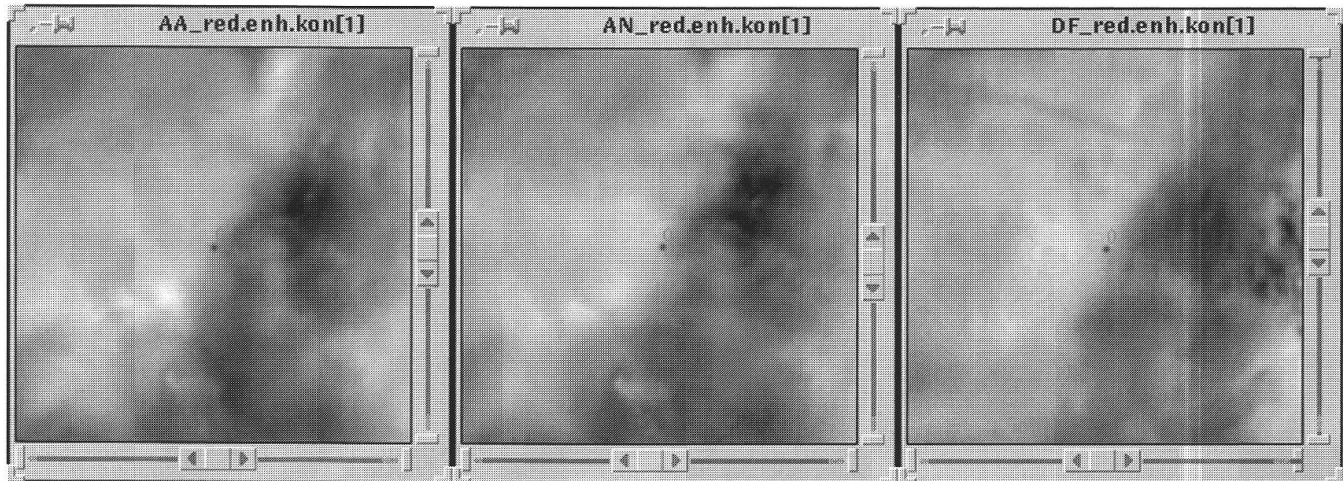


Figure 2: Matching difficulties between the MISR viewing angles (AA/AN to DF)

Probleme beim «matching» zwischen weiter auseinanderliegenden Aufnahmerichtungen von MISR (AA/AN zu DF)

Difficulté de trouver des points correspondants («matching») entre les directions d'acquisition de MISR (AA/AN à DF)

Photo: G. SEIZ

time delay between adjacent camera views is 45-60 seconds which results in a total delay between the DA and DF image of about 7 minutes. The four MISR spectral bands are centered at 446 (blue), 558 (green), 672 (red), and 866 nm (NIR). The data of the red band from all nine cameras and of the blue, green and NIR bands of the AN camera are saved in high-resolution, with a pixel size of 275 x 275 m; the data of the blue, green and NIR bands of the remaining eight cameras are stored in low-resolution, with a pixel size of 1.1 x 1.1 km. The operational data products from NASA are described in LEWICKI et al. (1999); the two products used for our investigations so far are the L1B2 Ellipsoid data (geolocated product) and the L2TC data (top-of-the-atmosphere/cloud product). With the development of a general sensor model for linear array sensors, we will start directly with the L1B1 data (unrectified product) in the near future.

Stereo CTH on a 1.1 x 1.1 km grid and CTW on a 70.4 x 70.4 km grid are provided within the operational MISR processing chain as part of the level 2TC product. The algorithms applied for the CTH and CTW retrieval are described in DINER et al. (1999) and HORVATH & DAVIES (2001). Important to note is that no subpixel matching algorithm is used and that the CTH and CTW for the high-resolution 1.1 x 1.1 km CTH product are not retrieved simultaneously, but in two steps: first, camera triplets (AN-BF-DF and/or AN-BA-DA) determine two CTW values for each 70.4 x 70.4 km with a histogram analysis; second, the matching results of AN-AF and/or AN-AA are converted into CTH

and corrected with the amount due to cloud motion within the 45 seconds between the acquisition of the two views. So, the principle of the algorithm is finally similar to our combined ATSR2-Meteosat-6 approach, except that only one instrument has to be used for the retrieval. The disadvantage in our approach with using two different satellites is obviously that the cloud objects can be slightly different in shape, so that the height correction is not applied correctly, for example at the cloud borders. Furthermore, differences in the wavelengths of the spectral channels used can also lead to errors in the correction, especially for multi-layer cloud situations. The disadvantage of the operational L2TC approach is that large discontinuities in the sparse CTW field can have a significant effect on the quality of the L2TC StereoHeight product, even if the AN-AF (and/or AN-AA) matching for their retrieval is very accurate and reliable. The MISR L2TC StereoHeight product can thereby suffer from some sort of blocking within the results. The 70.4 x 70.4 km CTW grid is probably too sparse, especially over land and mountainous terrain. It is very likely that the wind field is not homogenous within such a large grid cell, and as consequence, the CTH field is not accurately corrected. Another important factor for the quality of the CTW field and consequently the CTH field is the matching method. Operationally, the so-called NM matcher (DINER et al. 1999) is used for getting the triplets in the first step; only in the second step, the more reliable M23 matcher is applied. Some matching tests on this dataset have shown that, with applying the M23 matcher for both steps, the CTW results and the block-

ing problem can be improved significantly. Another possibility is an increase of the spatial resolution from 70.4 km to 35.2 km (HORVATH et al. 2002).

As own investigation, we started with the rectified MISR L1B2 Ellipsoid data, to test the LSM matching at this higher spatial resolution of 275 m versus ATSR2 and to evaluate if pixel-based triplet matching is possible with sufficient accuracy. The L1B2 Ellipsoid data were reduced to 8-bit and linearly stretched between the minimum and maximum value. As no a priori values of the cloud heights are given to the matching algorithm, a hierarchical matching procedure with 5 pyramid levels is applied so that the maximum possible parallax at the highest level is only a few pixels. Every pyramid level is enhanced and radiometrically equalized with a Wallis filter. Points with good texture are selected with the Förstner interest operator in the third pyramid level. The matching was done, as for the ATSR2 images, with the Multi-Photo Geometrically Constrained Matching Software package developed at our institute. The resulting x and y-parallaxes from three non-symmetric views (e.g. AN-AA-CF) are converted into CTH, along-track and cross-track wind components with the linear equations described in DINER et al. (1999). In the equations, the zenith angles from the Ancillary Geometric Product and the coefficients provided in the L1B2 metadata to calculate the exact acquisition time of each pixel are used. Especially between non-adjacent cameras, the matching is more difficult and will require some adaptations of the LSM algorithm to deal with shape changes and appearance/disappearance of cloud features. In particular the DF view is very delicate to be matched with the other views (Fig. 2); additionally, it is more problematic to assume that there is no vertical motion within 3.5 min (AN-DF) than within 45 seconds (AN-AF) or 92 seconds (AN-BF). With our current version of the LSM matching, the use of the AN, AF, BF and CF views (to benefit from the reliable sub-pixel accuracy of the matcher) seems to give better results, even if the separability of the parallax due to cloud height and the parallax due to cloud motion is mathematically superior when including the most oblique viewing angle(s) in the triplet (see HORVATH & DAVIES 2001, determinants of linear equation system for the different camera triplet combinations).

2.3 Geostationary stereo view: Meteosat-6/ Meteosat-7

The Meteosat-6 5min Rapid Scans during MAP together with the images from the operational Meteosat-7 satellite provided the possibility to stereo-view clouds over Europe with a geostationary satellite for the first time (SEIZ & BALTSAVIAS 2000). As the Meteosat satellites have a reversed scan mode (south-north) unlike all other meteorological satellites, their images

cannot be used for stereo mapping with other geostationary satellites. The first stereo configuration with two Meteosat satellites was achieved with Meteosat-5 and Meteosat-7 over the Indian Ocean, since the Meteosat-5 satellite was placed at 63° E for the INDOEX project (CAMPBELL & HOLMLUND 2000).

Unfortunately, the stereo configuration of Meteosat-6 and Meteosat-7 over Europe cannot be used for quantitative stereo analysis due to three reasons:

- Small longitude difference: Due to the small longitude difference of the two satellites, 0° and 9° W, compared to the satellite height, the base-to-height ratio is unfavorably low (~ 0.18).
- Scan synchronization: The two satellites are not synchronized, so that it is difficult to reach subpixel accuracy with matching, including the necessary motion correction. For the Meteosat-6 5min Rapid Scans, the time difference was about 1min, while for the new Meteosat-6 10min configuration, the time difference is more than 5min.
- Low image resolution: Given the spatial resolution of 2.5 x 4 km over Switzerland, small matching inaccuracies lead already to rather large CTH errors, which is even enhanced with the low base-to-height ratio.

Thus, in general, the stereoscopic effect is not pronounced. However, for vertically extended clouds, it is preferable to use the Meteosat quasi-synchronous stereo pairs for 3D visual cloud analysis.

3 Validation and combination with ground-based stereo analysis data

To validate the ATSR2 Stereo CTH and Meteosat-6 cloud motion winds during MAP, data from our newly developed ground-based stereo imager system (Fig. 3) (SEIZ et al. 2002) were used; the imager system was part of the MAP-Special Observation Period (SOP) composite observing system which was set up in the Rhine Valley, Switzerland, in autumn 1999. An improved version of the system has been installed at the Zurich-Kloten airport since September 2001.

Table 1 shows the exact acquisition times of ATSR2, Meteosat-6 and the ground-based stereo imager (skycam). The spatial extent of the skycam's overlap region depends on the installed lens (rectilinear or fish-eye) and the cloud height. In this case, the two cameras were equipped with rectilinear 18mm lenses (viewing angle 100°); with a mean cloud height of 10 km, an area of approximately 15 x 10 km can be used for the stereo-photogrammetric analysis. Table 2 shows the extracted skycam cloud-base height and motion, ATSR2 cloud top height and Meteosat-6 cloud top



Fig. 3: Camera system
Kamerasystem
Système de caméra

Photo: G. SEIZ

motion within the camera's field of view. The retrieved mean height in this area is 11.3 km above sea-level from the 11.0 μm channel and 10.2 km from the 0.87 μm channel. Obviously, only the upper layer is seen in the 11.0 μm channel, while in the 0.87 μm channel, cloud points both in the lower and higher layer are detected. In the ground-based images, two layers of clouds are clearly visible.

4 Conclusions

This paper has shown examples of satellite and ground-based stereo analysis of clouds. From satellites, there are various sensors currently available which can be used for stereo-photogrammetric cloud retrievals. For Stereo CTHs from a single polar-orbiter with only two viewing angles (e.g. ATSR2), it has proven to be absolutely necessary to correct the preliminary heights with CTW data from another source. Over land and mountainous regions, the cloud motion is most accurately derived from simultaneous images of a geostationary satellite. Over Europe, the Meteosat-6 Rapid Scan trials in 1999 (5min) and in 2000 (10min), and the operational Meteosat-6 10min Rapid Scans (since September 2001) are perfectly suited for this objective. The new MISR instrument and its products were presented as a promising alternative to derive CTH and CTW simultaneously with stereo-photogrammetric methods. The images from our new ground-based

Sensor	Acquisition time over Switzerland (Rhine Valley, 47.38 N/ 9.65 E)
ATSR2	forward: 10:16:30 nadir: 10:18:15
Meteosat -6	10:11/ 10:16/ 10:21/ etc.
Skycam	10:14/ 10:16/ 10:18/ etc.

Tab. 1: Overview of the acquisition times of the different sensors, 13th October 1999
Übersicht der Aufnahmezeiten der Sensoren, 13. Oktober 1999
Aperçu des heures d'acquisition des capteurs, 13 Octobre 1999

	ATSR2	Meteosat - 6	Skycam	
			Lower layer	Upper layer
Height [km asl]	0.87 μm : 10.2 ± 0.7 ¹ 11.0 μm : 11.3 ± 0.2 ¹	-	8.0 ± 0.11	10.9 ± 0.13
Motion [m/s]	-	19.3 ²	17.8	25.8
Motion direction[-	275 ²	274	276

¹Within box of 20 x 20 pixels

²Within box of 8 x 5 pixels

Tab. 2: Cloud parameters derived over Rhine Valley on 13th October 1999, from ATSR2, Meteosat-6 and the ground-based imager system (Skycam)

Abgeleitete Wolkenparameter aus ATSR2, Meteosat-6 und dem Boden-Kamerasystem (Skycam), Gebiet Rheintal, 13. Oktober 1999

Paramètres de nuages, dérivés de l'ATSR2, Meteosat-6 et du système de caméra terrestre (Skycam) dans la vallée du Rhin, 13 Octobre 1999

imager system (skycam) showed to be valuable validation data for vertically thin cloud situations.

In Cloudmap2, the validation of the satellite-based and ground-based stereo results will be continued, including the comparison with regional NWP model output fields. Furthermore, the combined data sets will be used for NWP assimilation tests on a very high spatial resolution (MeteoSwiss aLMo model with 50 x 50m grid width) and for 3D modelling and visualization of the cloud situation.

Acknowledgements

The Meteosat-6 and Meteosat-7 data were received from the EUMETSAT Archive Facility (MARF), the ATSR2 data via the ESA ATSR2 NRT service and the EOS-Terra MISR data (level 1B2 and level 2TC) were obtained from the NASA Langley Research Center Atmospheric Sciences Data Center. We thank Catherine Moroney and Akos Horvath, JPL, University of Arizona, for the reprocessing of the MISR L2TC dataset and for valuable input in the understanding of the L2TC products, and Chris Hansen, EUMETSAT, for information about the Meteosat-6 data. This work is funded by the Bundesamt für Bildung und Wissenschaft (BBW) within the EU-projects CLOUDMAP (BBW Nr. 97.0370) and CLOUDMAP2 (BBW Nr. 00.0355-1).

Literature

BALTSAVIAS, E.P. (1991): Multiphoto Geometrically Constrained Matching. – Ph. D. dissertation, Institute of Geodesy and Photogrammetry, ETH Zurich, Mitteilungen No. 49, 221 pp.

CAMPELL, G.C., & K. HOLMLUND (2000): Geometric cloud heights from Meteosat and AVHRR. – In: Proceedings Fifth International Winds Workshop, Lorne, Australia, February 28 to March 3, EUMETSAT, EUM P28.

DINER, D., DAVIES, R., DI GIROLAMO, L., HORVATH, A., MORONEY, C., MULLER, J.-P., PARADISE, S., WENKERT, D., & J. ZONG (1999): MISR Level 2 Cloud Detection and Classification. – = MISR Algorithm Theoretical Basis Documents, ATBD-MISR-07, NASA JPL.

EUMETSAT (2002): Rapid Scan Service (RSS). – <http://www.eumetsat.de/> 19.5.2003

FÖRSTNER, W. & E. GÜLCH (1987): A fast operator for detection and precise location of distinct points, corners, and centers of circular features. – In: Proc. ISPRS Intercommission Conf. on Fast Processing of Photogrammetric Data, Interlaken, Switzerland, June, 2-4: 281-305.

FUJITA, T.T. (1982): Principle of stereoscopic height computations and their applications to stratospheric cirrus over severe thunderstorms. – In: J. Met. Soc. Japan, 60, 1: 355-368.

GRÜN, A. (1985): Adaptive least squares correlation: a

powerful image matching technique. – In: S. Afr. J. of Photogrammetry, Remote Sensing and Cartography, 14, 3: 175-187.

HASLER, F. (1981): Stereographic observations from geosynchronous satellites: an important new tool for the atmospheric sciences. – In: Bull. Am. Met. Soc., 62, 2: 194-212.

HORVATH, A. & R. DAVIES (2001): Feasibility and error analysis of cloud motion wind extraction from near-simultaneous multiangle MISR measurements. – In: J. Atmos. Ocean. Technology, 18, April: 591-608.

HORVATH, A., DAVIES, R. & G. SEIZ (2002): Status of MISR cloud-motion wind product. – In: Proc. of 6th International Winds Workshop, May, 7-10, 2002, Madison, Wisconsin.

LEWICKI, S., CHAFIN, B., CREAN, K., GLUCK, S., MILLER, K. & S. PARADISE (1999): MISR Data Products Specifications. – = NASA JPL, http://eosweb.larc.nasa.gov/PRODOCS/misr/readme/dps_ne_icd.pdf 19.5.2003

LORENZ, D. (1985): On the feasibility of cloud stereoscopy and wind determination with the along-track scanning radiometer. – In: Int. J. Rem. Sens. 6, 8: 1445-1461.

MUTLOW, C. (1999): ATSR-1/2 User Guide, Issue 1.0, Rutherford Appleton Laboratory, Didcot, UK.

PRATA, A.J. & P.J. TURNER (1997): Cloud-top height determination using ATSR data. – In: Rem. Sens. Env. 59, 1: 1-13.

SEIZ, G. & E.P. BALTSAVIAS (2000): Satellite and ground-based stereo analysis of clouds during MAP. – In: EUMETSAT Conference Proceedings, Bologna, May 29 to June 2: 805-812.

SEIZ, G., BALTSAVIAS, E.P. & A. GRÜN (2002): Cloud mapping from the ground: use of photogrammetric methods. – In: Photogrammetric Engineering & Remote Sensing (PE & RS) 68, 9: 941-951.

WALLIS, R. (1976): An approach to the space variant restoration and enhancement of images. – In: Proc. of Symp. on Current Mathematical Problems in Image Science, Naval Postgraduate School, Monterey CA, USA, November, 10-14: 329-340.

YI, H., MINNIS, P., NGUYEN, L. & D.R. DOELLING (2001): A proposed multiangle satellite dataset using GEO, LEO and Triana. – In: Proc. of AMS, 11th Conference on Satellite Meteorology and Oceanography, October, 15-18, Madison, Wisconsin.

Summary: 3D Cloud Products for Weather Prediction and Climate Modelling

In this paper, the possibilities of satellite-based and ground-based stereoscopy of clouds are examined, with the objective to derive cloud top and cloud base heights and motion. These parameters are very important for a better description of clouds for nowcasting and numerical weather prediction models. For the satellite part, images of ATSR2 (on ERS-2) and MISR

(on EOS Terra) are used. As stereo image pairs from polar-orbiting satellites are never perfectly synchronous (time delay of some seconds between the image reception from the different viewing angles), the height error of the cloud top heights, introduced by the along-track motion component, is corrected with the cloud top winds extracted from Meteosat-6 and -7. For MISR, with nine viewing angles, this height correction is not needed when at least three images from non-symmetric cameras are used; then, it is possible to directly separate the along-track parallax (due to cloud height) from the along-track wind contribution (due to cloud motion). Our new ground-based imager system was operated in coincidence with an overpass of ERS-2 in October 1999. The ground measurements proved to be an interesting technique to validate satellite-based cloud top height and motion of vertically thin clouds and to additionally detect more detailed cloud features, which is particularly important for accurate nowcasting in mountainous terrain.

Zusammenfassung: 3D Wolkenprodukte für Wettervorhersage- und Klimamodelle

Der vorliegende Artikel befasst sich mit den Möglichkeiten der stereo-photogrammetrischen Auswertung von Satelliten- und Bodenmessungen von Wolken, mit dem Ziel, die Wolkenparameter «Wolkenhöhe» und «Wolkengeschwindigkeit» abzuleiten. Diese Wolkenparameter sind von entscheidender Bedeutung für eine bessere Erfassung der momentanen Wolkensituation für das Nowcasting und die numerischen Wettermodelle. Satellitengestützt werden Bilder von ATSR2 (auf ERS-2) und von MISR (auf EOS-Terra) analysiert. Da Stereopaare von einem Polarorbiter nie perfekt synchron sind (Verzögerung zwischen der Bildaufnahme der einzelnen Aufnahmerichtungen), muss der windbedingte Höhenfehler mit Wolkenwind-Daten, extrahiert aus Meteosat-6 und -7, korrigiert werden. Bei MISR mit neun Blickwinkeln ist diese Höhenkorrektur nicht nötig, sofern mindestens drei nicht symmetrische Kameras verwendet werden; dann können Wolkenhöhe und -geschwindigkeit in einem Schritt zusammen bestimmt werden. Unser neu entwickeltes, bodengestütztes Kamerasystem war simultan zu einem ERS-2 Überflug im Oktober 1999 in Betrieb. Die Bodenmessungen haben sich dabei als interessante Technik zur Validierung von Wolkenobergrenzenhöhe und -geschwindigkeit von vertikal dünnen Wolken herausgestellt, mit der zusätzlichen Möglichkeit, detailliertere Wolkenstrukturen zu erfassen, was vor allem für das Nowcasting in alpinem Gelände sehr wichtig ist.

Résumé: Produits 3D des nuages pour les modèles numériques de prévisions et les modèles climatologiques

L'article traite les possibilités de la stéréoscopie satellitaire et terrestre des nuages, avec le but de calculer les

paramètres «hauteur de nuage» et «vitesse de nuage». Ces paramètres sont très importants pour une description plus précise de la situation nuageuse, en vue du nowcasting et des modèles numériques. De la partie satellite, sont utilisées les images de l'ATSR2 (au bord de ERS-2) et du MISR (au bord de EOS-Terra). Car une paire d'images stéréo n'est jamais parfaitement synchronisée; l'erreur dans les hauteurs, introduite par le mouvement des nuages, doit être corrigée avec les données de vitesse des nuages, dérivées de Meteosat-6 et -7. Pour MISR avec neuf directions, cette correction n'est plus nécessaire si au moins trois images de caméras non-symétriques sont utilisées; la hauteur et la vitesse des nuages peuvent alors être calculées directement. Notre nouveau système de caméra terrestre était en opération pendant un survol de ERS-2 en Octobre 1999. Les mensurations terrestres ont montré qu'elles sont une source valable pour valider la hauteur et la vitesse de nuages très minces (en direction verticale) et pour détecter des structures de nuage plus détaillées, qui sont importantes en particulier pour le nowcasting dans le terrain montagneux.

Teaching of Geography – pertinent questions

- What possibilities do satellite and ground-based stereo-photogrammetric analysis of clouds offer? Which cloud parameters can be retrieved?
- Which satellite and ground instruments are currently available in stereo configuration for cloud property retrievals? What are the processing steps?

- What are the benefits of these new 3D cloud products for numerical weather prediction and climate modelling?
- What are the goals of the Cloudmap 2 program?

Dipl.-Geogr. **Gabriela Seiz**, Institut für Geodäsie und Photogrammetrie, ETH Hönggerberg, CH-8093 Zürich, und MeteoSchweiz, Krähbühlstrasse 58, CH-8044 Zürich.

e-mail: gseiz@geod.baug.ethz.ch

Dr. **Emmanuel P. Baltasvias**, Institut für Geodäsie und Photogrammetrie, ETH Hönggerberg, CH-8093 Zürich.

e-mail: manos@geod.baug.ethz.ch

Prof. Dr. **Armin Grün**, Institut für Geodäsie und Photogrammetrie, ETH Hönggerberg, CH-8093 Zürich.

e-mail: agruen@geod.baug.ethz.ch

Manuskripteingang/received/manuscript entré le
7.2.2003

Annahme zum Druck/accepted for publication/accepté
pour l'impression: 5.6.2003